Journal of Physics: Conference Series **141** (2008) 012004 doi:10.1088/1742-6596/141/1/012004

The 'KER' effect in the double photoionization of H_2

J. Colgan[1], T. J. Reddish[2], A. Huetz[3], P. Bolognesi[4], L. Avaldi[4], M. Gisselbrecht[3], M. Lavollée[3], and M. S. Pindzola[5]

[1]Theoretical Division, Los Alamos National Laboratory, Los Alamos, NM 87545, USA
[2]Department of Physics, University of Windsor, 401 Sunset Ave, Ontario, Canada, N9B 3P4
[3]CNRS-Université Paris Sud, UMR8624, Laboratoire d'interaction du rayonnement X avec la matière, Bat. 350, Centre d'Orsay, 91405, Orsay, France
[4]CNR -IMIP Area della Ricerca di Roma 1, CP 10 00016 Monterotondo Scalo, Italy
[5]Department of Physics, Auburn University, Auburn, AL 36849, USA

E-mail: jcolgan@lanl.gov

Abstract. Recent experimental and theoretical work examining the double photoionization of H_2 has uncovered surprising changes in the fully differential cross sections as a function of the kinetic energy released to the protons (which is equivalent to different internuclear separations of the molecule). We describe the recent joint theoretical and experimental investigations which have uncovered the physical reasons for this phenomenon. We show that the observed variations are solely due to the ϵ_Σ component of the polarization vector along the molecular axis. Our conclusions are supported by further investigations of the photoionization of H_2^+, in which similar dramatic variations in the photoelectron angular distributions for the $\sigma_g \rightarrow \sigma_u$ transition are found as the internuclear separation is varied. The angular distributions for the $\sigma_g \rightarrow \pi_u$ transition show little dependence on the internuclear separation.

1. Introduction

Double photoionization of molecular hydrogen has been an intense field of study in recent years. This research has built on successful studies of double photoionization of He, where it has been demonstrated that experiment and several theoretical approaches are in very good agreement for all measurable quantities. H_2 is a more complex system to study than He, due to the two-center Coulomb potential in which the electrons move. This allows purely molecular effects, such as vibration and rotation, to exist, as well as greatly complicating the electron dynamics. In double photoionization, where both electrons are suddenly ejected from the molecule, which subsequently 'explodes', recent experimental studies have uncovered changes in the fully differential cross sections (FDCS) of the escaping electrons as a function of the molecular orientation [1, 2], work which was supported by theoretical calculations [3, 4, 5]. Furthermore, the FDCS was also found to be sensitive to the kinetic energy released (KER) to the exploding protons, which is equivalent to a sensitivity to the internuclear separation of the molecule at the time the electrons escape. This surprising result was first explored by Weber *et al* [6], and further investigated theoretically by Horner *et al* [7], who found that the KER effect was related to the different variations of the Σ and Π contributions to the cross section as a function of the KER (or, equivalently, the internuclear separation, R).

A very recent joint experimental and theoretical study [8] found that the KER effect was solely present in the Σ contribution to the cross section, and was enhanced at certain molecular

orientations due to sensitivities in the cross term contribution to the FDCS. Furthermore, an analogy to the single photoionization of H_2^+ was made, for which the resulting angular distributions also show some sensitivity to the internuclear separation [9]. In this progress report, we present further details of this study and discuss the similarities between double photoionization of H_2 and single photoionization of H_2^+.

2. Method

The FDCS measurements were obtained using 100% linearly polarized light from the Elettra synchrotron in conjunction with a momentum imaging apparatus; further details are given elsewhere [2, 10, 11]. The photon energy was 76.09 eV, $\sim$ 25 eV above the nominal threshold at the equilibrium internuclear separation ($1.4a_0$) and near the peak maximum of the total double photoionization cross section. The observed FDCSs are compared to those obtained using the time-dependent close-coupling (TDCC) method, which has been described in detail previously [5, 12]. To study the KER dependence, a TDCC calculation is performed at different values of R. A TDCC calculation is also made for each final M symmetry accessible by a single-photon transition (i.e. $M = 0, \pm 1$, where M is the total magnetic quantum number in the body frame). When constructing FDCSs, the amplitudes which result from these calculations must be added coherently, and are weighted by appropriate factors for a given molecular orientation [Ref. [5], Eq. (11)]. Thus, the total contribution to the FDCS consists of a Σ ($M = 0$) component, a Π ($M = \pm 1$) component, and cross terms arising when the total amplitude is squared to obtain the FDCS. Convolution over experimental solid angles can easily mask or smear out the KER-dependent FDCS. An advantageous feature of momentum imaging methods is the ability to select the experimental bandwidths in the data analysis, and is completely decoupled from the data acquisition. Although $\sim$ 1.1 million four particle coincidence events were obtained in this study [2], careful attention was still needed in choosing the critical variables over which one can convolute large ranges without compromising the direct observation of KER effects. To compare with experiment, the TDCC FDCSs are also convoluted, by performing calculations for a detailed grid of angles and energies over the range of experimental bandwidths, and then appropriately averaging the results. We also examined the TDCC FDCS as a function of the various bandwidths to determine which variables are most sensitive to the convolution procedure. It was found that θ_N (the polar angle between the molecular orientation and the polarization direction) was the most critical variable to minimize, and that the other variables were insensitive to convolution, even over fairly large ranges. Hence we selected $\theta_N = \pm 10^o$ but with large values of the other bandwidths and with the electron energies $E_1 = E_2 = 12.5 \pm 10$ eV, in both the experimental measurements and in the TDCC convoluted calculations.

3. Results and Discussion

In figure 1 we present FDCSs at three different molecular orientations as indicated, for two different molecular internuclear separations, i.e. for two different KER values. In all cases the first electron is ejected at 90° with respect to the polarization direction. Integration over R as a continuous variable is not performed in the TDCC averaging, thus preventing a precise comparison with the experimental data on an absolute scale. The orientations shown in figures 1a ($\theta_N = 90^o$) and 1c ($\theta_N = 0^o$), allow us to isolate the Π and Σ amplitudes respectively. As R is decreased from 1.6 a_0 to 1.2 a_0 (moving from left to right), we find that the shape of the FDCS for the Π orientation shows little change. For the Σ orientation a small change in the shape of the FDCS results from the decrease in R. At smaller R the lobes of the FDCS are pushed even further away from the θ_1 direction for this case (where θ_1 is the angle between one of the outgoing electrons and the polarization direction, as defined in Fig. 1 of [8]).

However, for the intermediate orientation presented in figure 1b ($\theta_N = 20^o$), we find a dramatic variation in the FDCS as R is decreased. At the larger R most of the yield is in

the 4th quadrant, whereas when R is smaller, the yield in the 3rd and 4th quadrants is almost identical.

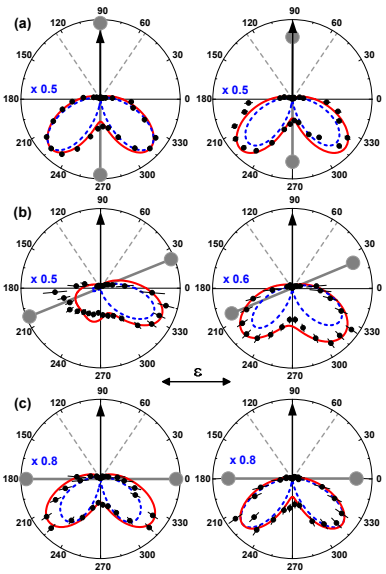

Figure 1. (color online) H_2 FDCSs in the 'coplanar' geometry for three 'in plane' molecular orientations, θ_N = (a) 90°, (b) 20°, and (c) 0°, all with the first electron at $\theta_1 = 90^o$ and for $E_1 = E_2 = 12.5 \pm 10$ eV. Two KER values, (a,b) 16.5 (left) and 23.5 eV (right), and (c) 16 (left) and 24 eV (right), corresponding to approximately R = 1.6, 1.2 a_0, respectively, are shown for each θ_N angle. The angular step in θ_2 is 10°. The dotted lines indicate a dead sector, symmetric with respect to the vertical axis, for the detection of the second electron. The bandwidths are: $\Delta E_{KER} = \pm 2$ eV (a,b), 4 eV (c); $\Delta\theta_N = \pm 10^o$; $\Delta\theta_1 = \pm 20^o$; $\Delta\phi_{12} = \pm 45^o$; $\Delta\phi_{1N} = \pm 60^o$ (not relevant in bottom line). The experimental data are arbitrarily normalized to the TDCC results convoluted over the experimental bandwidths (solid); unaveraged TDCC results for the stated (θ_1, θ_N) values (dashed) have the scaling factors indicated.

A further example of the KER effect is presented in figure 2. In this case we consider a different electron ejection angle of $\theta_1 = 60^o$, and show two molecular orientations, $\theta_N = 20^o$ and $\theta_N = 160^o$. For both of these cases, as R is varied the FDCS changes dramatically. The variation is observed in the unaveraged TDCC calculations, as well as in the TDCC calculations convoluted over experimental bandwidths. In all cases the averaged calculations are in excellent agreement with experiment.

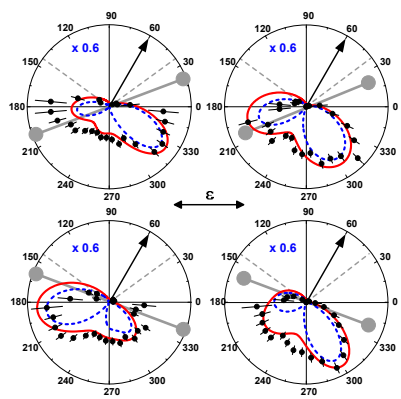

Figure 2. (color online) As in Fig. 1(b), but for molecular orientations $\theta_N = 20^o$, 160°; all with $\theta_1 = 60^o$.

Why does the FDCS depend so critically on R? Furthermore, as also shown by Horner *et al* [7] for asymmetric energy sharings, why does an angle of $\theta_N \sim 20^o$ seem so critical to observe these dramatic KER effects? Some insight into these questions can be found by looking at the various contributions which make up the FDCS, namely the Σ, Π components and their cross terms. Such information reveals the importance of each term. In figure 3 we show these individual components for two molecular orientations, again $\theta_N = 160^o$ (left) and $\theta_N = 20^o$ (right), for electron ejection angles of $\theta_1 = 20^o$ and 60° respectively.

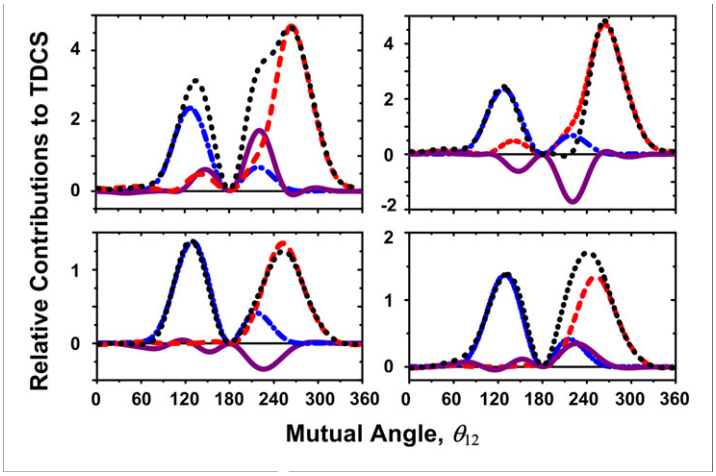

Figure 3. (color online) The relative contributions to the TDCC FDCS (dot) from the pure Π (dash-dot) and Σ (dash) contributions, and their cross term (solid), for (θ_1, θ_N) values of (20°, 160°) left and (60°, 20°) right, and for $R = 1.6a_0$ (upper) and $1.2a_0$ (lower). Here $E_1 = E_2 = 10$ eV. At these (θ_1, θ_N) values the peaks at $\theta_{12} \sim 130^o$ and $\sim 250^o$ in the total FDCS are primarily due to the Π and Σ contributions, respectively; see text for discussion.

We see immediately that, at these orientations, both the Σ and Π components make significant contributions to the total FDCS, and that *only* the Σ component shows a change in shape with R. Moreover, changes in sign and shape of the cross term contribution with R results in constructive and destructive interference between the two components, amplifying the small changes with R of the Σ component. We now understand why the molecular orientation angle of $\sim 20^o$ is critical to observing the KER effects; it is only at around these angles where the Σ and Π relative contributions are approximately equal, so allowing for significant interference effects between the components. The KER effect also appears to be present for all electron energy sharing conditions.

The immediate question which follows such analysis is: why does only the Σ component show a sensitivity to R? In fact, the work of Horner *et al* [7] showed that the behaviors of the Π and Σ contributions to the total and single differential cross sections were quite different as a function of R. The Π contribution decreases monotonically as R increases, whereas the Σ contributions exhibits a shallow minimum near the equilibrium internuclear separation. This change is conveniently expressed by the variation of the ion asymmetry β_N parameter with R. The present TDCC calculations are in very good agreement with the exterior complex-scaling (ECS) calculations of Horner *et al* [7], and the R-averaged TDCC value of -0.73 is in very good agreement with the experimentally observed value of -0.75 ± 0.1 [2]. The dominance of the Π component results in a negative β_N which varies with R due to the different R dependencies of the Π and Σ components.

In fact, similar behavior exists for the related process of the single photoionization of H_2^+. A recent study of Colgan *et al* [9] showed that the σ and π contributions to the total cross section also behave differently with R. As also found in the double photoionization of H_2 case, and as demonstrated in figure 4 for H_2^+, the π contribution to the total photoionization cross section decreases monotonically with R, whereas the σ contribution exhibits a shallow minimum at intermediate R.

The angular distributions arising from photoionization of H_2^+ also show dramatic variations with R. In figure 5 we present the angular distributions for photoionization of H_2^+ by a photon of energy 65 eV, as a function of R. The left plot shows the case where the molecule is aligned parallel to the polarization axis (i.e. a pure σ component) and the right plot shows the case where the molecule is perpendicular to the polarization axis (a pure π component). As R is increased, the σ angular distributions change dramatically with R in both shape and magnitude, where as the π distributions show little sensitivity to R.

To understand this variation of the cross section for the σ component, we can consider the

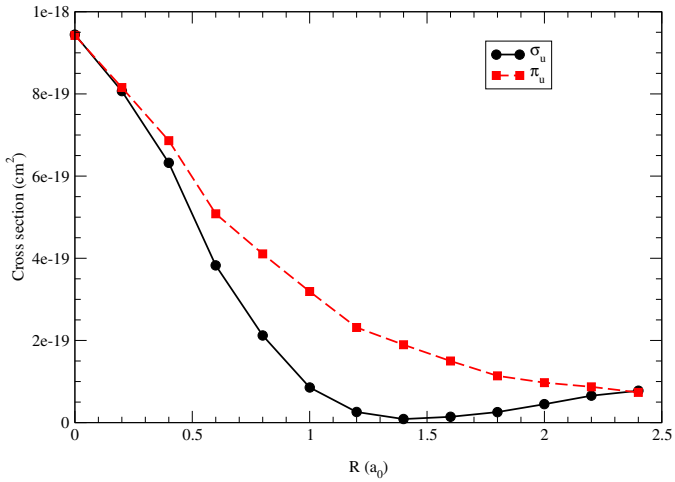

Figure 4. Total photoionization cross section for H_2^+ as a function of the internuclear separation, R, for a photon energy of 65 eV, for molecular orientations aligned parallel to the polarization axis (σ_u final state; black solid line) and perpendicular to the polarization axis (π_u final state; red dotted line).

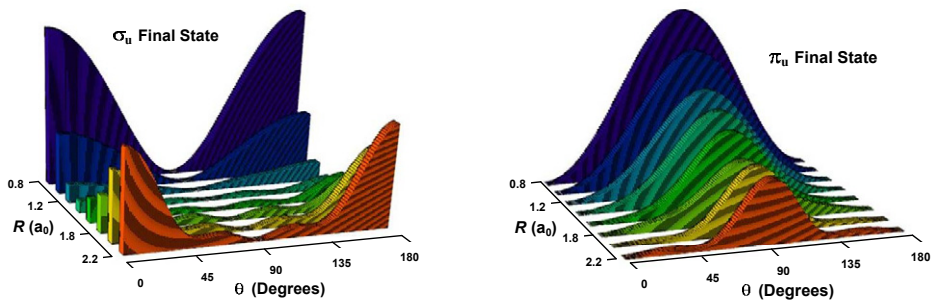

Figure 5. Angular distributions for photoionization of H_2^+ as a function of R, for a fixed outgoing electron energy of 10 eV. The left panel shows a pure σ orientation (parallel alignment) and the right panel shows a pure π orientation (perpendicular alignment).

individual partial wave components which make up the photoionization cross sections. In figure 6 we show, for three R values as indicated, the cross section contributions when only up to $l = 1$ components are retained in the cross section (red dashed line), and when up to $l = 3$ (p, f) components are retained (green dot-dashed line), for the σ (upper panels) and π cases (lower panels). In this case we fix the photoelectron energy to be 10 eV. For the σ case, as R increases, the p contribution, which had been completely dominant at smaller R, decreases sharply, so that at $R = 1.8a_0$, the f component dominates the shape and magnitude of the photoionization cross section. No such variation occurs for the π case, which is dominated at all R by the p component. Similar distributions are found for the case where the photon energy, rather than the photoelectron energy, is fixed [9].

This disappearance of the p contribution to the photoionization cross section is due to an almost complete cancellation between the positive and negative portions in the $1s\sigma_g \rightarrow kp\sigma_u$ dipole matrix element at this R and k value (where k is the momentum of the outgoing photoelectron). Such a cancellation, which may also be referred to as a Cooper minimum [13], was first recognized over fifty years ago by Bates *et al* [14]. It is this cancellation which causes the minimum in the σ component of the total photoionization cross section of H_2^+, and the dramatic variation with R of the angular distributions for the σ case. Such a cancellation does not occur for the π component for these R values at low energies. A much more complete discussion of this Cooper minimum for H_2^+, for a wide range of R and k values, was recently

published [15] and was also noted by Fernández *et al* [16].

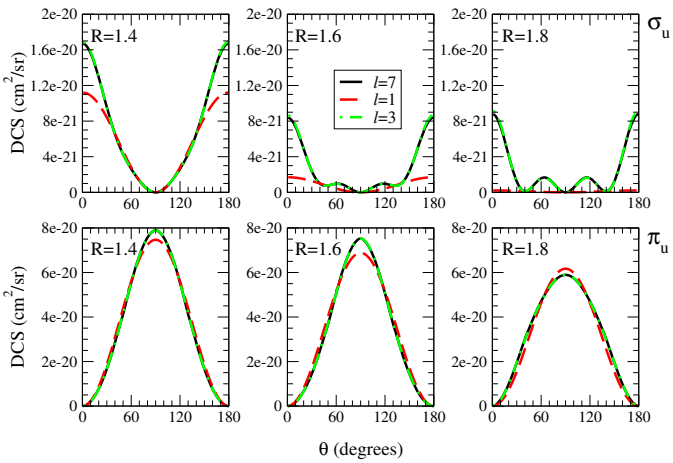

Figure 6. Partial wave contributions to the differential cross sections for photoionization of H_2^+ for a fixed photoelectron energy of 10 eV, for three internuclear separations R as indicated. The upper panels show the cross sections for a final σ_u state (parallel orientation) and the lower panels show the cross sections for a final π_u state (perpendicular orientation). The red dashed lines and green dot-dashed lines show the contributions including up to $l = 1$ and $l = 3$ respectively. The full calculations, indicated by the solid black line, include up to $l = 7$.

Since we now understand the reason for the R dependence of the σ component of the single photoionization cross section of H_2^+, and noting that the σ and π contributions to the total cross section for the photoionization of H_2^+ and to the double photoionization of H_2 behave similarly with R, it is tempting to ascribe the same reasoning to the R dependence of the FDCS for double photoionization of H_2. However, caution is required, since double photoionization of H_2 is a much more complex process than single photoionization of H_2^+, and since the shapes of the FDCS are often dominated by electron correlation effects between the two outgoing electrons. Furthermore, the Cooper minimum phenomena is strictly a one-electron effect. However, we can study the partial wave convergence of the double photoionization of H_2. In figure 7 we return to a FDCS first presented experimentally in figure 3 of Gisselbrecht *et al* [2], which was later shown to be in good agreement with TDCC calculations (figure 3 of [5]). In this orthogonal geometry the first electron is ejected out of the page, and the molecule is oriented (a) out of the page (so only the Π component contributes) and (b) along the polarization axis (only the Σ component contributes). We show only the unaveraged TDCC calculations (which are also in excellent agreement with ECS calculations [4]), and test calculations which include partial wave contributions up to $l_{\max} = 1$, 2, 3, and 4, as indicated (where $l_{\max}$ in this case refers to the maximum value of any of the $l_1 l_2$ orbital angular momenta of the two outgoing electrons). For the pure Π case ($\theta_N = 90^o$) of panel (a), we find that the addition of successively higher partial waves does not change the shape of the FDCS, and that by including up to $l_{\max} = 3$, the shape and magnitude of the FDCS is quite well converged. For the pure Σ case of panel (b), the addition of partial waves up to and above $l_{\max} = 3$ does change the shape of the FDCS, giving the final cross section extra structure. In addition, we see that, even by $l_{\max} = 4$, the magnitude of the cross section is still not completely converged. By isolating some of the $l = 3$ components (solid purple line in panel (b)), we confirm that the extra structure in the final cross section does arise from such high partial waves. We also note that the magnitude of the cross section for the pure Σ case is much smaller than for the pure Π cases.

4. Conclusion

To summarize, we have further explored the KER effect in the double photoionization of H_2. The dependence of the FDCS on the internuclear separation R is found to occur only in the Σ

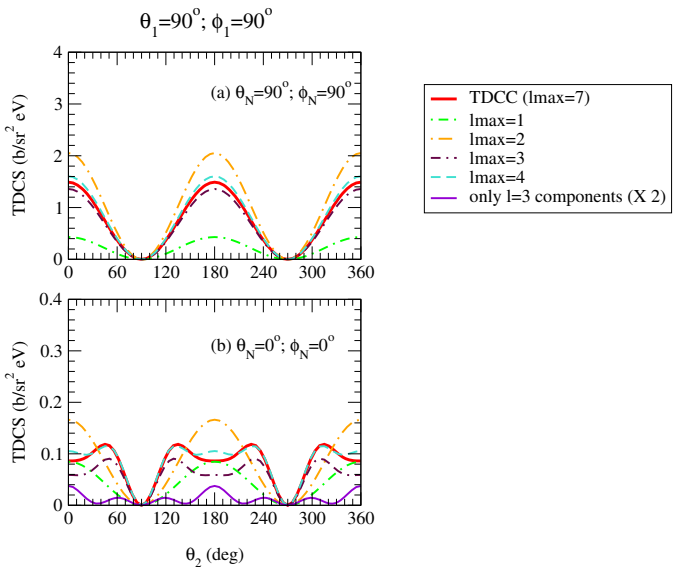

Figure 7. TDCC calculations of the FDCS for molecular orientations as indicated, for the orthogonal geometry, with the first electron perpendicular to the plane of the figure (i.e. $\theta_1 = 90^o$ and $\phi_1 = 90^o$), which contains the second electron (i.e. $\phi_2 = 0^o$), and for $E_1 = E_2 =$ 10 eV. The thick red lines are the complete TDCC calculations, and the various dashed and dotted lines show the contributions from truncating the calculations at various partial wave values as indicated. The solid purple line shows part of the $l = 3$ contribution, and is multiplied by 2 for clarity.

contribution to the FDCS, and is amplified through the cross terms when molecular orientation is such that the Σ and Π contributions are approximately of equal magnitude. The Σ contribution to the FDCS is found to be more sensitive to the number of partial waves retained in the calculations. We also find that in the analogous process of single photoionization of H_2^+, where the KER effect is also observed for the σ component and not for the π component, a Cooper minimum in the $1s\sigma_g \rightarrow kp\sigma_u$ contribution to the dipole matrix element largely explains the KER effect in the σ component.

Acknowledgments
We would like to thank the staff at Elettra and the Gas Phase beamline team for their invaluable assistance, and EU, NSERC and UoW for their financial support. Some of this work was performed under the auspices of the US DOE through Los Alamos National Laboratory (LANL) and through NSF and DOE grants to Auburn University. Computational work was carried out at NERSC in Oakland, CA, the NCCS in Oak Ridge, TN, and through LANL Institutional Computing Resources.

[1] Weber T *et al* 2004 *Phys. Rev. Letts.* **92** 163001
[2] Gisselbrecht M *et al* 2006 *Phys. Rev. Letts.* **96** 153002
[3] Vanroose W, Martín F, Rescigno T N and McCurdy C W 2005 Science **310** 1787-1789
[4] Vanroose W, Horner D A, Martín F, Rescigno T N and McCurdy C W 2006 *Phys. Rev. A* **74** 052702
[5] Colgan J, Pindzola M S and Robicheaux F 2007 *Phys. Rev. Letts.* **98** 153001
[6] Weber T *et al* 2004 *Nature* **431** 437-441; 2006 **443** 1014
[7] Horner D A, Vanroose W, Rescigno T N, Martín F and McCurdy C W 2007 *Phys. Rev. Letts.* **98** 073001
[8] Reddish T J, Colgan J, Bolognesi P, Avaldi L, Gisselbrecht M, Lavollée M, Pindzola M S and Huetz A 2008 *Phys. Rev. Lett.* **100** 193001
[9] Colgan J, Huetz A, Reddish T J and Pindzola M S 2008 *J. Phys. B* **41** 085202
[10] Gisselbrecht M *et al* 2005 *Rev. Sci. Instrum.* **76** 013105
[11] Gisselbrecht M, Lavollée M, Huetz A, Bolognesi P, Avaldi L, Seccombe D P and Reddish T J 2006 *J. Phys.: Conf. Ser.* **88** 012006
[12] Colgan J, Pindzola M S and Robicheaux F 2004 *J. Phys. B* **37** L377
[13] Carlson T A *et al* 1986 *Z. Phys. D* **2** 309-318
[14] Bates D R, Öpik U and Poots G 1953 *Proc. Phys. Soc. A* **66** 1113-1123
[15] Della Picca R, Fainstein P D, Martiarena M L and Dubois A 2008 *Phys. Rev. A* **77** 022702
[16] Fernández J, Fojón O, Palacios A and Martín F 2007 *Phys. Rev. Lett.* **98** 043005